Minimizing crosstalk in three-axial induction magnetometers

Asaf Grosz, Eugene Paperno, Shai Amrusi, and Tal Szpruch
Department of Electrical and Computer Engineering, Ben-Gurion University of the Negev, 84105 Beer-Sheva, Israel

(Received 29 August 2010; accepted 10 October 2010; published online 22 December 2010)

A model for crosstalk in three-axial induction magnetometers has been developed theoretically and verified experimentally. The effect of crosstalk on the magnetometer accuracy has been analyzed. It has been found that the inevitable crosstalk in the transverse coils has two components: one due to the applied magnetic flux and the other due to the secondary flux produced by the electric current in the longitudinal coil. The first component has a constant magnitude. The phase of the second component, relative to the first one, is nearly 180° at low frequencies, 90° at resonance, and 0° at high frequencies. Its magnitude approaches zero at low frequencies, has the maximum at resonance, and then drops off by a factor equal to the coils' quality factor and approaches the first component value. As a result, the crosstalk due to the applied flux is dominant at low frequencies. At a frequency just below the resonance, the crosstalk is very low, if no magnetic feedback is applied. Just above the resonance, the crosstalk reaches the maximum because of the rapid increase in the secondary flux. Applying a strong enough magnetic feedback nearly flattens the crosstalk amplitude response. However, an undesirable effect of the feedback is that it significantly increases the minimum crosstalk value. A very low crosstalk at a single frequency can be beneficial for magnetometers tuned to a narrow frequency band. It can also be beneficial for wide-band magnetometers to measure their mechanical orthogonality with a minimum effect of crosstalk. © *2010 American Institute of Physics*. [doi:10.1063/1.3509392]

I. INTRODUCTION

Induction magnetometers[1–7] should comprise at least three orthogonal coils[1–4] (see Fig. 1) to measure a magnetic field in three-dimensional space. An important characteristic of a three-axial magnetometer is its orthogonality: a field applied along a magnetometer coil should *not* be sensed by the transverse coils. Imperfect orthogonality degrades the magnetometer accuracy of measuring the direction and magnitude of the applied field.

Two main factors affecting the magnetometer orthogonality are the mechanical precision of assembling the coils and the crosstalk between them. Even in a perfectly precise assembly, the transverse coils may still be sensitive to the applied flux as well as to the secondary flux generated by the electric current flowing in the longitudinal coil (see Fig. 2).

Magnetic crosstalk may be absent in a multicoil assembly: more than three coils,[4] for example, six can be arranged absolutely symmetrically, as shown in Fig. 1(a), where the coils in each couple are connected in series. In such a configuration, both the applied, Φ_a, and secondary, Φ_s, fluxes generate zero average fluxes in the transverse coils. As a result, there is no crosstalk between the magnetometer channels: a nonzero output is generated only by the longitudinal coils.

Employing, however, a large number of coils increases not only the magnetometer complexity but also its size and, hence, decreases its accuracy of measuring inhomogeneous fields. For these reasons, typical induction magnetometers[1–4] comprise only three coils.

In a triple-coil assembly, the crosstalk is inevitable. As one can see from Fig. 1(b), three orthogonal coils cannot be arranged absolutely symmetrically. As a result, the transverse coils do become sensitive both to the applied and secondary fluxes (see Figs. 3 and 4). Figure 3 shows that in an asymmetrical assembly, the transverse cores provide a shortcut for the applied flux, thus, a part of it flows through them around the longitudinal core. As a result, the applied field causes a primary flux not only in the longitudinal coil but also in the transverse ones. Figure 4 shows that the transverse cores shunt the secondary flux as well and, therefore, conduct a part of it.

Depending on frequency, the secondary flux in the longitudinal coil can be much greater than the primary flux and the corresponding crosstalk component can be very strong. In some experiments, for example, we operated three-axial induction magnetometers at resonance, where they are most sensitive, and measured about 50% total crosstalk. Applying magnetic feedback had not helped bringing the crosstalk below 5%, no matter what was the amount of the feedback.

Having found no treatment of the crosstalk in literature, we are bridging this gap in the present work by analyzing the crosstalk in triple-coil induction magnetometers and its effect on the magnetometer accuracy. Our aim was to build a theoretical model to predict and minimize the crosstalk strength.

The developed model shows that the crosstalk can be surprisingly strong, especially at resonance. It also shows that, on the other hand, the crosstalk can be negligibly weak at a frequency just below the resonance. Our model shows as well to what extent the crosstalk is affected by magnetic feedback. To validate the crosstalk model, a triple-coil magnetometer has been built and tested.

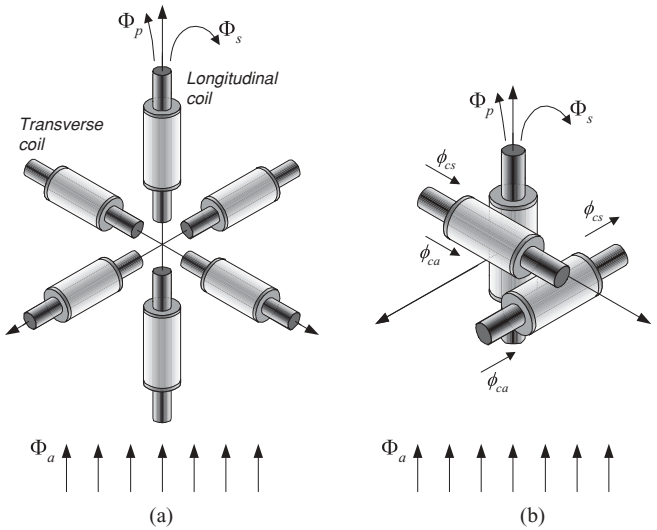

FIG. 1. Three-axial induction magnetometers: (a) a crosstalk free configuration, (b) a configuration with a crosstalk between the magnetometer coils. Φ_p and Φ_s are the primary and secondary fluxes in the longitudinal coil. ϕ_{ca} and ϕ_{cs} are the crosstalk components due to the applied, Φ_a, and secondary fluxes, respectively.

II. THEORETICAL MODEL

A. Crosstalk due to the applied and secondary fluxes

Let us consider the equivalent electrical circuit of a magnetometer channel with magnetic feedback (see Fig. 2). We assume that the channel coil is aligned along the applied flux. The total crosstalk can be found as follows, neglecting the reverse crosstalk caused by the secondary fluxes produced by the transverse coils (the validity of such an approximation is given in the Appendix),

$$\phi_{c\Sigma} = \frac{\Phi_{c\Sigma}}{\Phi_p} = \phi_{ca1} + \frac{\phi_{cs1}\Phi_s}{\Phi_p} = \phi_{ca1} + \phi_{cs1}\phi_s = \phi_{ca} + \phi_{cs}, \quad (1)$$

where $\Phi_{c\Sigma}$ is the total flux in a transverse coil, Φ_p is the primary flux in the longitudinal coil, ϕ_{ca1} is the flux due to the applied field that causes a unit primary flux, ϕ_{cs1} is the flux due to a unit secondary flux, ϕ_s is the relative secondary flux, and ϕ_{ca} and ϕ_{cs} are the crosstalk components due to the applied and secondary fluxes, respectively.

From Fig. 2, Φ_s can be found as follows:

$$\Phi_s = \frac{1}{N}(LI + MI_f) = \frac{1}{N}\left(L\frac{v_o}{A}j2\pi fC + M\frac{v_o}{R_f}\right), \quad (2)$$

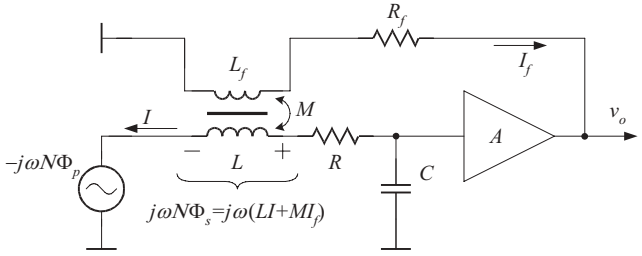

FIG. 2. Equivalent electrical circuit of the longitudinal magnetometer channel.

where N is the number of the coil turns, L is the coil self inductance, I is the coil current, M is the mutual inductance between the magnetometer and feedback coils, I_f is the feedback coil current, v_o is the channel output voltage, A is the voltage gain of the preamplifier, C is the coil capacitance, and R_f is the feedback resistor value.

Assuming that R_f is much greater than the other part of the impedance at the feedback coil terminals,

$$v_o = -j2\pi fN\Phi_p \frac{A}{1 + j2\pi f\left(RC + M\frac{A}{R_f}\right) - CL(2\pi f)^2}. \quad (3)$$

Substituting Eq. (3) into Eq. (2) gives us the relative secondary flux

$$\phi_s = \frac{\Phi_s}{\Phi_p} = \frac{1}{1 + \frac{1}{j2\pi f\frac{AM + j2\pi fR_fLC}{R_f(1 + j2\pi fRC)}}}. \quad (4)$$

The total longitudinal coil flux ϕ_Σ relative to Φ_p can be found as follows:

$$\phi_\Sigma = \frac{\Phi_\Sigma}{\Phi_p} = \frac{\Phi_p + \Phi_s}{\Phi_p} = 1 + \phi_s. \quad (5)$$

The total relative flux ϕ_Σ in Eq. (5) differs from the crosstalk $\phi_{c\Sigma}$ in Eq. (1) only in the weighting factors ϕ_{ca1} and ϕ_{cs1}. Therefore, it is instructive to analyze the behavior of ϕ_Σ to understand the behavior of $\phi_{c\Sigma}$.

The ϕ_{ca1} and ϕ_{cs1} factors depend on a large set of the coil parameters, such as the cores' aspect ratios, the shortest distances between the cores, the cores' magnetic permeability, and the relative length of the coils. It is difficult to describe the ϕ_{ca1} and ϕ_{cs1} factors analytically for a general case.

Fortunately, they can readily be found for a specific coil assembly with the help of commercially available three-dimensional finite-element applications.

To illustrate the above theoretical model, we will use ϕ_{ca1} and ϕ_{cs1} computed (see Figs. 3 and 4) for an inductive magnetometer assembled from the coils shown in Fig. 5. For this specific coil assembly, $\phi_{cp1} = 2.02\%$ and $\phi_{cs1} = 3.03\%$.

The assembly parameters are as follows. The shortest distances between the cores' axes are 16 mm. The core material is a MnZn ferrite with a 2000 relative magnetic permeability. The other coil parameters are: $L = 17.46$ H, $R = 6.38$ kΩ, $C = 5.26$ nF, $M = 0.042$, the coil self-resonant frequency $f_0 = 525$ Hz, and the coils' quality factors $Q = 9.03$. The preamplifier gain $A = 1000$.

B. Frequency dependence of the relative total flux

We will analyze here the frequency dependence of the relative total flux in the longitudinal coil for different amounts of magnetic feedback. Figure 6 illustrates the effect of the feedback on the frequency response of the magnetometer channel, and Figs. 7 and 8 show the secondary and total relative fluxes, respectively, with and without feedback.

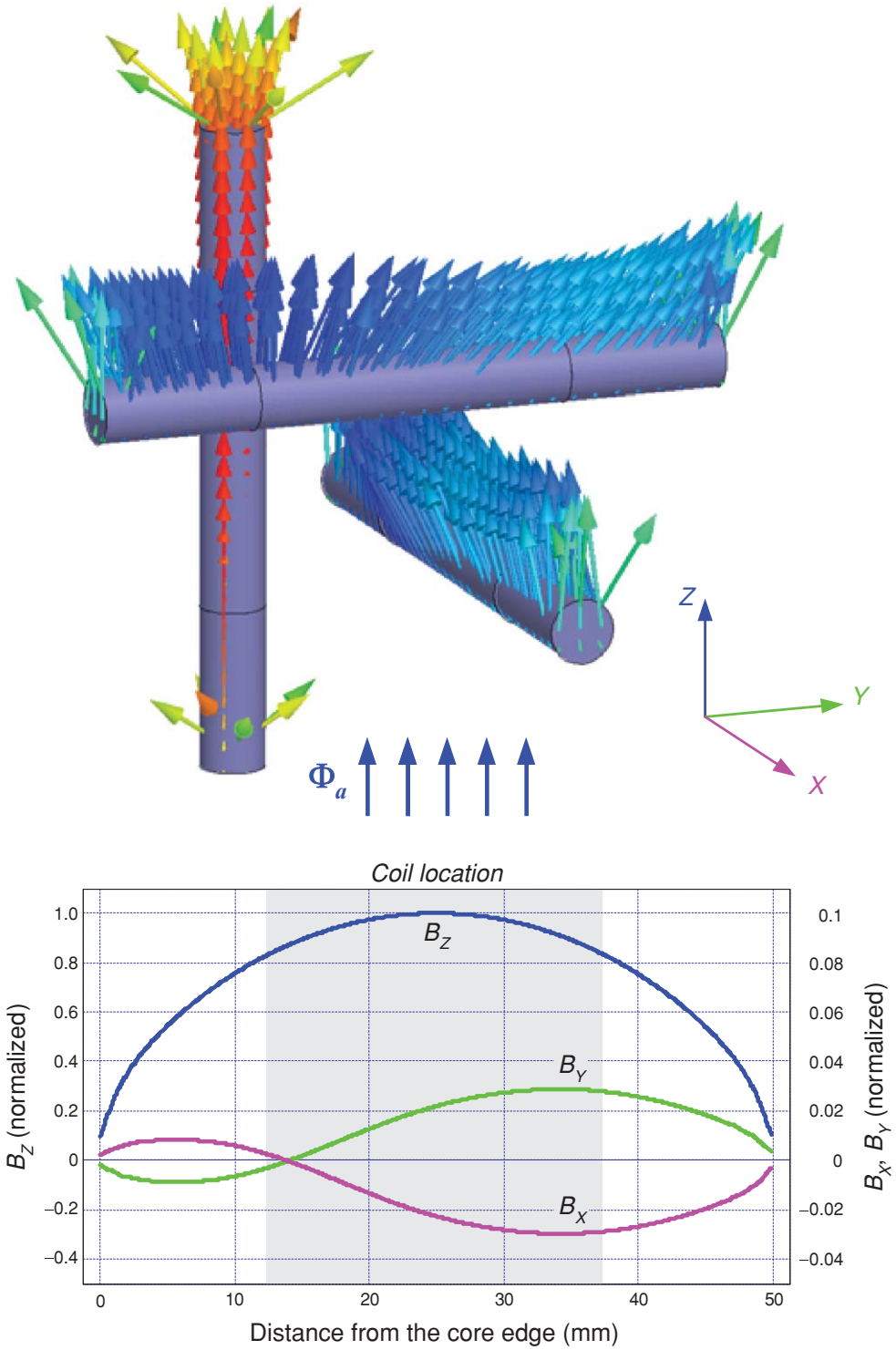

FIG. 3. (Color online) Crosstalk due to the applied flux Φ_a (a uniform magnetic field is applied along *Z*-core): (top) magnetic induction within the cores, (bottom) magnetic induction along the core axes. The coils are not shown. Note that there are net magnetic fluxes within the transverse cores. Relative to the primary flux in the longitudinal coil, the crosstalk $\phi_{ca1} = 2.02\%$. The coil dimensions are given in Fig. 5. (Calculated with Maxwell 13.0.)

One can see from Fig. 7 that below the coil self-resonant frequency, ϕ_s without feedback is nearly opposite to the normalized primary flux ϕ_p. As a result, the total relative flux ϕ_Σ in Fig. 8 has a minimum at a frequency

$$f_{\phi\Sigma\,\min} = f_0 \frac{\sqrt{2}}{\sqrt{3+\sqrt{1+24\pi^2(f_0RC)^2}}}, \tag{6}$$

just below f_0, where ϕ_s and ϕ_p are nearly equal in magnitudes.

At low frequencies, ϕ_Σ approaches ϕ_p, because ϕ_s rapidly decreases below resonance. At resonance, ϕ_s exceeds ϕ_p by a factor of Q, and ϕ_Σ reaches the maximum just above f_0. At high frequencies, ϕ_Σ reaches a value of 2 because ϕ_s approaches unity and is in phase with ϕ_p (see Fig. 7).

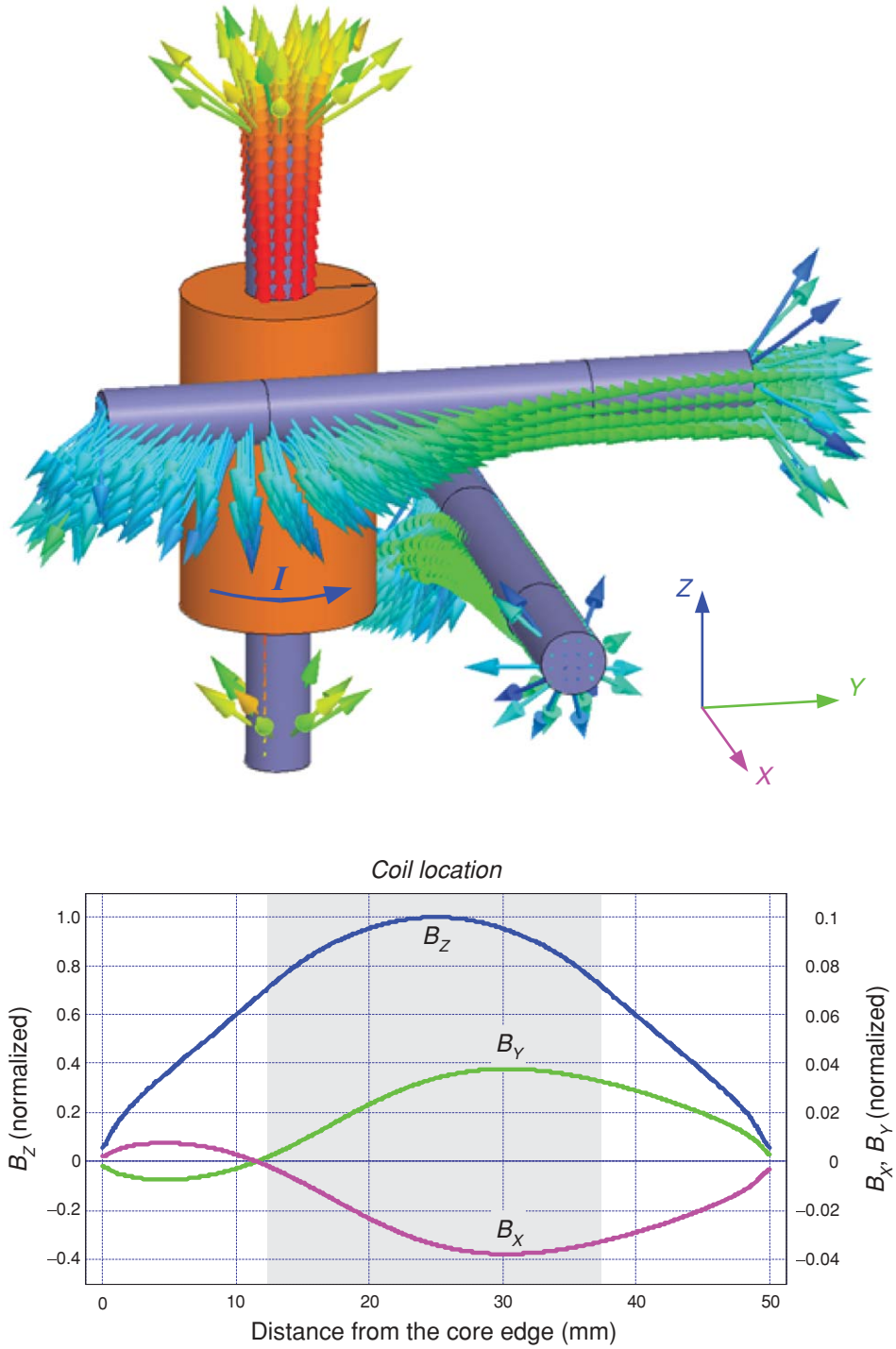

FIG. 4. (Color online) Crosstalk due to the secondary flux Φ_s (an electric current is applied to *Z*-coil): (top) magnetic induction within the cores, (bottom) magnetic induction along the core axes. Only *Z*-coil is shown. Note that the secondary field causes fluxes in the transverse cores. These fluxes are directed similarly to the fluxes caused by the applied field in Fig. 3. Relative to the secondary flux in the longitudinal coil, the crosstalk $\phi_{cs1} = 3.03\%$. The coil dimensions are given in Fig. 5. (Calculated with Maxwell 13.0.)

Magnetic feedback although significantly decreases ϕ_Σ at resonance, it, on the other hand, significantly increases ϕ_Σ at $f_{\phi\Sigma\min}$. A strong feedback (low R_f) also increases ϕ_Σ at low frequencies.

C. Frequency dependence of the crosstalk

The behavior of the total flux suggests a similar behavior of the crosstalk: the minimum crosstalk without feedback will be reached at a frequency where ϕ_{ca} and ϕ_{cs} significantly compensate each other. At low frequencies, ϕ_{ca} will dominate, $\phi_{c\Sigma}$ will nearly approach $Q\phi_{cs1}$ just above the resonance and approach $\phi_{ca1} + \phi_{cs1}$ at higher frequencies. Magnetic feedback will significantly decrease the maximum value of the crosstalk and increase its minimum value.

To illustrate the above, we calculate in Fig. 9 and Table I the total crosstalk $\phi_{c\Sigma}$. The crosstalk reaches the minimum at 331 Hz, which is about 10% below $f_{\phi\Sigma\min} = 370$ Hz,

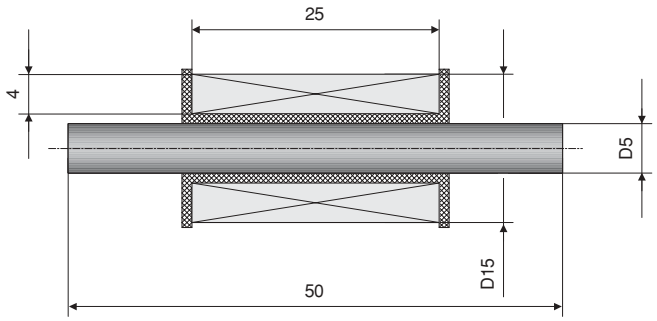

FIG. 5. Magnetometer coil.

and reaches the maximum at 529 Hz, which is about 1% above the resonance. At resonance $\phi_{c\Sigma} = 27.4\% \approx Q\,\phi_{cs1}$. Strong enough magnetic feedback squeezes the crosstalk between the ϕ_{ca1} and $\phi_{ca1} + \phi_{cs1}$ limits.

D. Effect of crosstalk on the magnetometer accuracy

To evaluate the effect of the crosstalk on the magnetometer accuracy, we have calculated the magnetometer outputs for a field vector rotating in such a way that its tip draws in space a spherical spiral. The following approximations have been obtained for the maximum uncertainty in the measured field direction (in degrees) and for the maximum relative uncertainty in the field magnitude:

$$\varphi_{\max} \approx 85\phi_{c\Sigma} - 40\phi_{c\Sigma}^2 + 35\phi_{c\Sigma}^3, \tag{7}$$

$$\delta R_{\max} \approx \begin{cases} +\phi_{c\Sigma}100\% \\ -2\phi_{c\Sigma}100\% \end{cases}. \tag{8}$$

Considering Eqs. (7) and (8), the total crosstalk found in Sec. II C (see Table I) causes the magnetometer inaccuracy given in Table II.

III. EXPERIMENT

To validate the theoretical model of the crosstalk, we have built and tested a three-axial induction magnetometer. The parameters of the magnetometer coils and the preamplifier match the parameters given in Sec. II.

TABLE I. Total crosstalk $\phi_{c\Sigma}$.

Frequency (Hz)	Low	331	$f_0 = 525$	529	High
			No feedback		
Crosstalk (%)	2.02	0.23	27.43	27.70	5.05
			With feedback ($R_f = 70$ kΩ)		
Crosstalk (%)	2.02	4.44	5.10	5.10	5.05

In our experiments, one of the magnetometer coils was aligned along the applied field, and the outputs of all the magnetometer channels were measured. To calculate the crosstalk (see Fig. 10), the amplitude responses of the transverse channels were divided by that of the longitudinal channel. One can see from Fig. 10 that a very good agreement between the theory and experiment has been obtained.

IV. CONCLUSION

A model for crosstalk in three-axial induction magnetometers has been developed theoretically and verified experimentally. The model shows that the crosstalk ϕ_{ca1} due to the applied flux is dominant at low frequencies. At a frequency just below the resonance, the crosstalk is very low, if no magnetic feedback is applied. This is because of a significant mutual compensation of the primary and secondary fluxes. Just above the resonance, the crosstalk reaches the maximum because of the increase in the secondary flux. At high frequencies, the crosstalk approaches $\phi_{ca1} + \phi_{cs1}$. Applying a strong enough magnetic feedback nearly flattens the crosstalk amplitude response and keeps it between the ϕ_{ca1} and $\phi_{ca1} + \phi_{cs1}$ limits. However, an undesirable effect of the feedback is that it significantly increases the minimum crosstal value.

A very low crosstalk, close to 0.2%, obtained at a single frequency can be beneficial for magnetometers tuned to a narrow frequency band. It can also be beneficial for wideband magnetometers to measure their mechanical orthogonality with a minimum effect of crosstalk.

Our numerical simulations also show that decreasing the shortest distance between the cores' axes, from 16 to

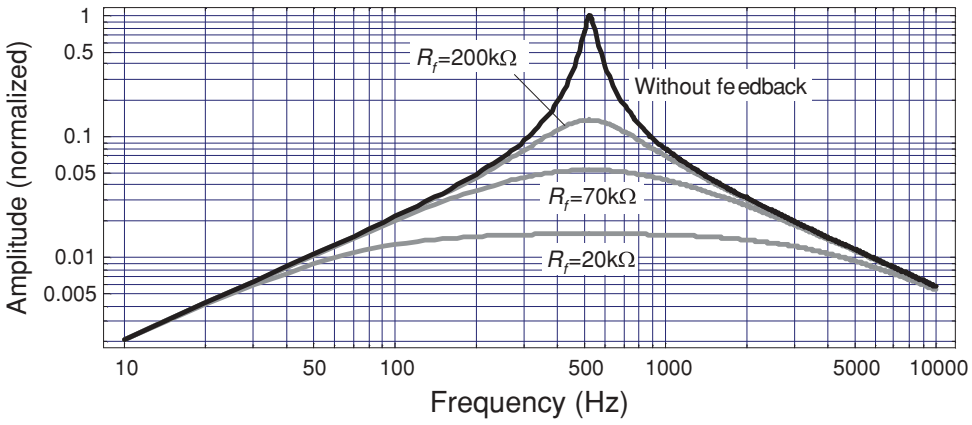

FIG. 6. (Color online) Magnetometer frequency response.

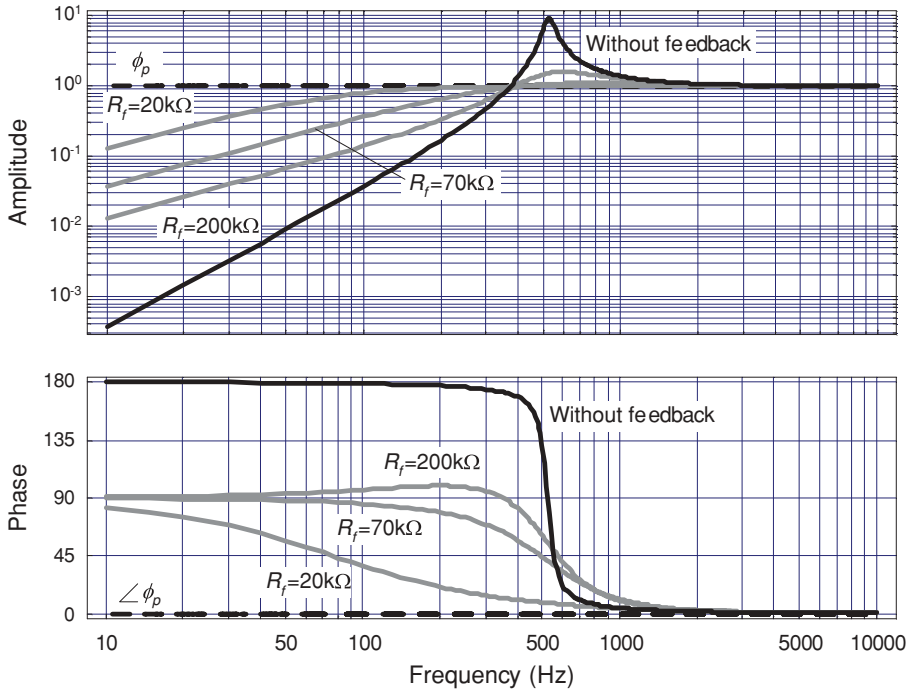

FIG. 7. (Color online) The secondary relative flux ϕ_s as a function of frequency and the amount of feedback.

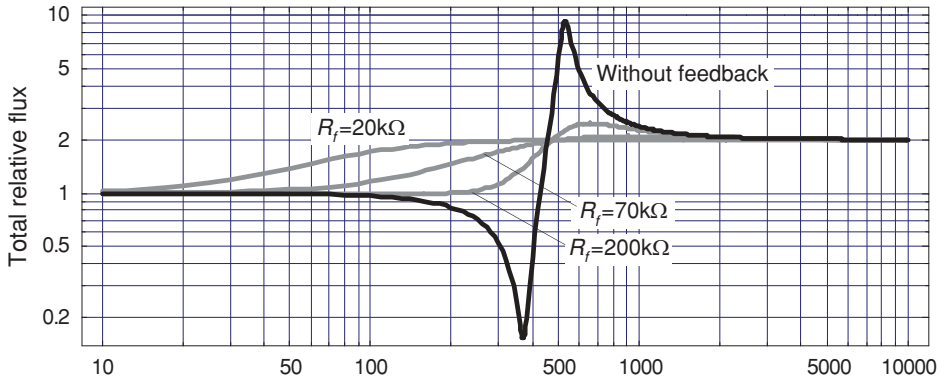

FIG. 8. (Color online) The total relative flux ϕ_Σ as a function of frequency and the amount of feedback.

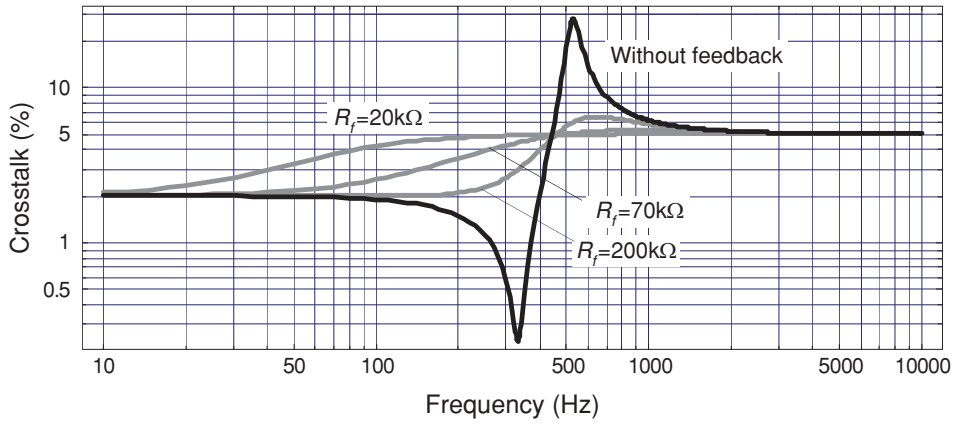

FIG. 9. (Color online) The total crosstalk $\phi_{c\Sigma}$ as a function of frequency and the amount of feedback.

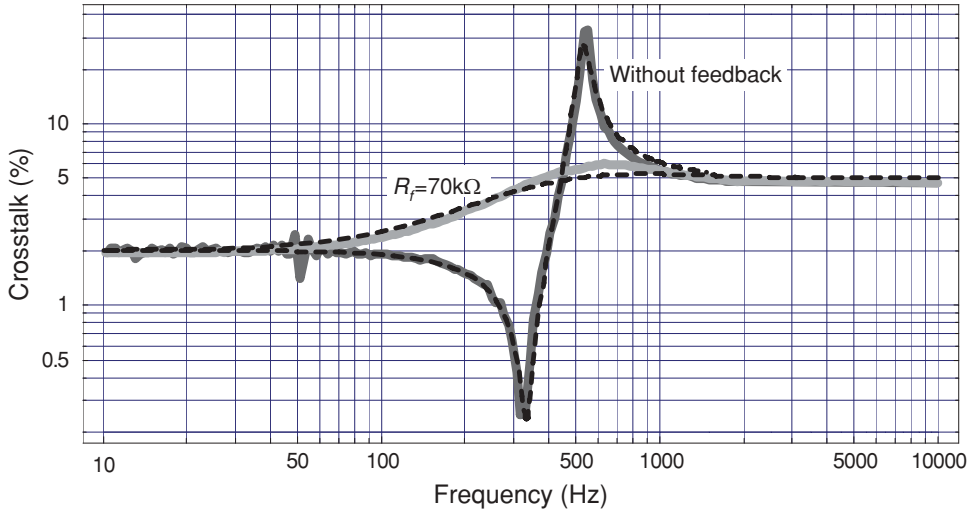

FIG. 10. (Color online) Total magnetometer crosstalk $\phi_{c\Sigma}$: a comparison between the theory and the experiment. The dashed and solid curves represent the theoretical and experimental data, respectively.

8 mm, reduces the ϕ_{ca1} and ϕ_{cs1} factors by half. This leaves, however, much less space for the coils, thus, decreasing their sensitivity. Doubling the distances between the cores' axes has a similar effect. Doubling the core lengths reduces ϕ_{ca1} by half and ϕ_{cs1} by third. However, this significantly increases the magnetometer size and degrades its accuracy of measuring inhomogeneous fields. The cores' magnetic permeability has a little effect on the crosstalk: increasing the permeability from 10^3 to 10^5 increases the ϕ_{ca1} and ϕ_{cs1} factors by less than 15%. Increasing the coils' lengths also has a little effect on the crosstalk: the crosstalk reduction is less than 15%.

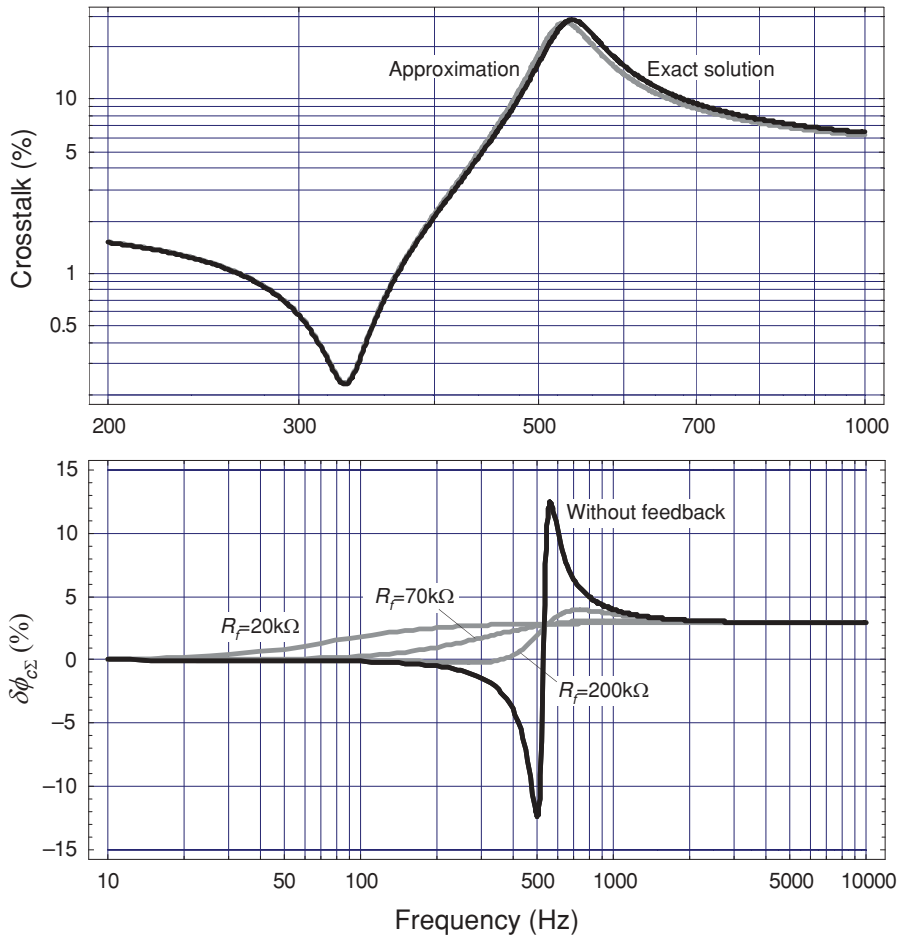

FIG. 11. (Color online) Exact and approximate crosstalk: (top) a comparison of the crosstalk values for the case of no magnetic feedback, (bottom) the relative error of the approximation.

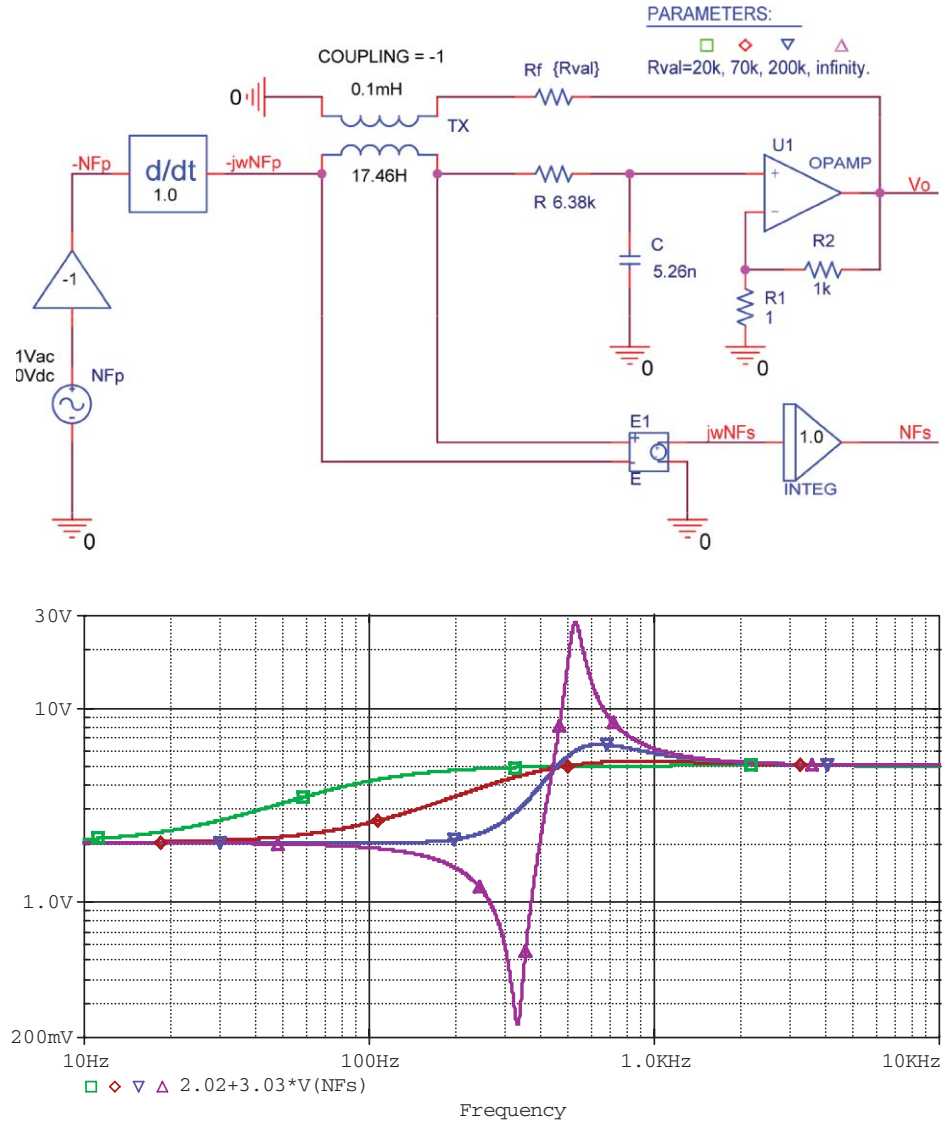

FIG. 12. (Color online) Crosstalk simulation in SPICE: (top) design schematic, (bottom) the total crosstalk $\phi_{c\Sigma}$ as a function of frequency and the amount of feedback (volts correspond to %). (The letter "F" stands for "Φ".)

The suggested approach to studding crosstalk in three-axial induction magnetometers can also be helpful for understanding and describing crosstalk in other types of magnetometers, such as air-core search coils,[8] fluxgates,[9–12] magneto-impedance magnetometers,[13] metal detectors,[14] etc.

TABLE II. Maximum uncertainties caused by the crosstalk.

Frequency (Hz)	Low	331	$f_0 = 525$	529	High
			No feedback		
Field direction	1.7°	0.2°	21.0°	21.2°	4.2°
Field magnitude (%)	+2.0	+0.2	+27.4	+27.7	+5.1
	−4.0	−0.4	−54.9	−55.4	−10.1
			With feedback ($R_f = 70$ kΩ)		
Field direction	1.7°	3.9°	4.2°	4.2°	4.2°
Field magnitude (%)	+2.0	+4.44	+5.1	+5.1	+5.05
	−4.0	−8.88	−10.2	−10.2	−10.1

ACKNOWLEDGMENTS

This work was supported in part by Analog Devices, Inc., National Instruments, Inc., and the Ivanier Center for Robotics Research and Production Management.

APPENDIX: CONSIDERING THE REVERSE CROSSTALK

Considering the crosstalk caused by the secondary fluxes, Φ'_{st}, produced by the transverse coils, Eq. (4) can be rewritten as follows:

$$\Phi'_s = (\Phi_p + 2\phi_{cs1}\Phi'_{st})T(f), \tag{A1}$$

where

$$\Phi'_{st} = (\phi_{ca1}\Phi_p + \phi_{cs1}\Phi'_s + \phi_{cs1}\Phi'_{st})T(f), \tag{A2}$$

and

$$T(f) = \frac{1}{1 + \dfrac{1}{j2\pi f \dfrac{AM + j2\pi f R_f LC}{R_f(1 + j2\pi f RC)}}}. \quad \text{(A3)}$$

Solving Eqs. (A1) and (A2) for Φ'_s and Φ'_{st}, the relative secondary fluxes in the longitudinal and transverse coils can be obtained:

$$\phi'_s = \frac{\Phi'_s}{\Phi_p} = \frac{1 + \phi_{cs1}(2\phi_{ca1} - 1)T(f)}{1 - \phi_{cs1}[1 + 2\phi_{cs1}T(f)]T(f)} T(f), \quad \text{(A4)}$$

$$\phi'_{st} = \frac{\Phi'_{st}}{\Phi_p} = \frac{\phi_{ca1} + \phi_{cs1}T(f)}{1 - \phi_{cs1}[1 + 2\phi_{cs1}T(f)]T(f)} T(f). \quad \text{(A5)}$$

The crosstalk can be found as the ratio of the primary fluxes in the transverse and longitudinal coils:

$$\phi'_{c\Sigma} = \frac{\Phi'_{pt}}{\Phi'_{pl}} = \frac{\phi_{ca1}\Phi_p + \phi_{cs1}\Phi'_s + \phi_{cs1}\Phi'_{st}}{\Phi_p + 2\phi_{cs1}\Phi'_{st}} = \frac{\phi_{ca1} + \phi_{cs1}\phi'_s + \phi_{cs1}\phi'_{st}}{1 + 2\phi_{cs1}\phi'_{st}}. \quad \text{(A6)}$$

The relative error of the approximation neglecting the reverse crosstalk caused by the secondary fluxes produced by the transverse coils can now be found as follows:

$$\delta\phi_{c\Sigma} = \frac{|\phi'_{c\Sigma}| - |\phi_{c\Sigma}|}{|\phi'_{c\Sigma}|} 100\%. \quad \text{(A7)}$$

For the three-axial magnetometer analyzed in this work, the exact (A6) and approximate (1) models of the crosstalk are compared in Fig. 11. This figure shows that model (1) is quite accurate. The relative difference between the maximum values of the exact and approximated crosstalk is only 3.4% if no magnetic feedback is applied. The exact crosstalk reaches the maximum at 537 Hz, compared to 529 Hz for the approximate crosstalk. The magnitude of the approximation error is about 13% just below and above the resonance and rapidly decreases for other frequencies. Applying magnetic feedback decreases $|\delta\phi_{c\Sigma}|$ below 4% in the entire frequency range.

The simplified approach used in the present work, besides providing a clearer insight into the crosstalk mechanism, allows one to very quickly and conveniently estimate the crosstalk in SPICE.

To illustrate this, we show in Fig. 12 a SPICE simulation, where the crosstalk is found by simply integrating the voltage across the magnetometer coil inductance. According to Fig. 2, this yields $N\Phi_s$. For the input voltage source value equal to 1 V (this is equivalent to $N\Phi_p = 1$ W), the relative secondary flux $\phi_s = \Phi_s/\Phi_p = N\Phi_s$, and the crosstalk can be found as $\phi_{c\Sigma} = \phi_{ca1} + \phi_{cs1}N\Phi_s$, or, in our case, $\phi_{c\Sigma} = 2.02 + 3.03\, N\Phi_s$ (%).

[1] H. C. Séran and P. Fergeau, Rev. Sci. Instrum. **76**, 044502 (2005).
[2] J. B. Cao, Z. X. Liu, J. Y. Yang, C. X. Yian, Z. G. Wang, X. H. Zhang, S. R. Wang, S. W. Chen, W. Bian, W. Dong, Z. G. Zhang, F. L. Hua, L. Zhou, N. Cornilleau-Wehrlin, B. de Laporte, M. Parrot, H. Alleyne, K. Yearby, O. Santolík, and C. Mazelle, Ann. Geophys. **23**, 2803 (2005).
[3] A. Roux, O. Le Contel, C. Coillot, A. Bouabdellah, B. de la Porte, D. Alison, S. Ruocco, and M. C. Vassal, Space Sci. Rev. **141**, 265 (2008).
[4] J. C. Dupuis, "Optimization of a 3-axis induction magnetometer for airborne geophysical exploration," M.Sc. thesis, University of New Brunswick, 2001.
[5] E. Paperno and A. Grosz, J. Appl. Phys. **105**, 07E708 (2009).
[6] A. Grosz, E. Paperno, S. Amrusi, and E. Liverts, J. Appl. Phys. **107**, 09E703 (2010).
[7] C. Coillot, J. Moutoussamy, P. Leroy, G. Chanteur, and A. Roux, Sens. Lett. **5**, 167 (2007).
[8] S. Tumanski, Meas. Sci. Technol. **18**, R31 (2007).
[9] P. Ripka, *Magnetic Sensors and Magnetometers* (Artech House, Norwood, MA, 2001).
[10] P. Ripka and A. Tipek, *Modern Sensors Handbook* (ISTE, London, 2007).
[11] E. Paperno, E. Weiss, and A. Plotkin, IEEE Trans. Magn. **44**, 4018 (2008).
[12] I. Sasada and K. Goleman, IEEE Trans. Magn. **42**, 3276 (2006).
[13] K. Kawashima, T. Kohzawa, H. Yoshida, and K. Mohri, IEEE Trans. Magn. **29**, 3168 (1993).
[14] H. Ewald and H. Krueger, "Inductive sensors and their application in metal detection," Proceedings of the 1st International Conference on Sensing Technology, Palmerston North, New Zealand, 21–23 November 2005.